iomac
International Operational Modal Analysis Conference

11th International Operational Modal Analysis Conference

20 - 23 May 2025 | Rennes, France

Post-processing of fiber optic sensors data with consideration of strain transfer for distributed strain measurements

Mira Kabbara [1], *Xavier Chapeleau* [2], *Qinghua Zhang*[3] *and Frédéric Bourquin*[4]

[1] COSYS-SII/I4S, Université Gustave Eiffel, Inria, 44340 Bouguenais, France, mira.kabbara@univ-eiffel.fr
[2] COSYS-SII/I4S, Université Gustave Eiffel, Inria, 44340 Bouguenais, France, xavier.chapeleau@univ-eiffel.fr
[3] COSYS-SII/I4S, Université Gustave Eiffel, Inria, 35042 Rennes, France, Qinghua.Zhang@inria.fr
[4] Université Gustave Eiffel, 77420 Champs-sur-Marne, France, frederic.bourquin@univ-eiffel.fr

ABSTRACT

In recent years, fiber optic sensors are widely used in structural health monitoring due to their high-spatial resolution distributed measurements. However, strain transfer through protective coatings of the sensors can distort measurements, especially in high strain gradients. To correct this, mathematical models of strain transfer have been developed and validated through numerical simulations and experiments. Recovering the actual strain profile involves inverting these models, particularly a 1D second-order differential equation derived from a 3D model. This equation, subject to boundary conditions, must be solved repeatedly for efficient numerical inversion. Given the high sampling frequencies of fiber optic sensors, fast algorithms are crucial for real-time applications such as vibration analysis. This paper proposes an efficient method to solve the 1D strain transfer equation and its inverse problem. By enabling rapid post-processing of strain measurements, this approach aims to enhance the application of fiber optic sensors in vibration analysis and structural health monitoring.

Keywords: fiber optic sensors, distributed strain measurements, strain transfer model, inverse problem

1. INTRODUCTION

Structure monitoring has gained significant importance in recent years, attracting considerable research attention[1]. In this field, various sensors are employed to gather data on parameters that indicate the health condition of structures. Among these technologies, distributed fiber optic sensors stand out for their ability to provide continuous monitoring along an entire structure[2]. Modern distributed fiber optic sensors for dynamic strain monitoring are achieving higher spatial resolution, with current capabilities

reaching down to the centimeter scale [3]. Ongoing advancements in fiber optic technology and signal processing are expected to further enhance spatial resolution, potentially reaching millimeter-scale accuracy, with high-frequency interrogation enabling real-time data acquisition in future applications. However, efficiently processing the data at these high speeds remains a key challenge. Data processing for strain measurements with fiber optic sensors must account for the strain transfer phenomenon, which causes the actual strain in the host material to differ from the measured strain. This phenomenon occurs because the optical fiber sensor—composed of a core (sensitive element), optical cladding, and protective coatings—can experience attenuation and deformation in the intermediate layers. Correcting this discrepancy is crucial to ensuring accurate and reliable monitoring results. To address this, several studies have developed a simplified 1D model that links the actual strain profile in the host material to the measured profile[4–6]. This model uses a second-order differential equation with a parameter, known as the strain-lag parameter, that incorporates the geometric and mechanical properties of the cable and its installation within the structure. Many studies have focused on deriving analytical solutions for this model, particularly when the actual strain is expressed as a simple function[7, 8], others have validated the direct problem numerically through 3D finite element simulations, comparing the 1D model results with the 3D output at the core of the fiber optic sensor[9].

The purpose of this article is to propose a method to recover the actual strain profile in the host material from the measured strain profile, which is fast enough to be compatible with vibration analysis for structural health monitoring, based on the aforementioned 1D model. This model is a differential equation whose direct numerical solution allows the measured strain profile to be calculated from the actual strain profile. Therefore, it is the inverse problem that needs to be solved, which is inherently ill-conditioned. The 1D strain transfer model is first presented, then a new method is proposed to solve its second-order differential equation. This method decomposes the equation into two first-order equations, which are then solved as initial value problems with their initial conditions set to zero. The two initial value problems are solved in two opposite directions (right to left or left to right) in order to ensure the numerical stability of each solution. Two additional terms are introduced so that the total solution satisfies the boundary conditions specified at both ends of the considered interval. This approach ensures numerical stability, prevents error accumulation, and is fast enough for real-time solution of the inverse problem in the context of vibration analysis. The resolution of the inverse problem is based on minimizing an error criterion iteratively: in each iteration, the actual strain profile estimate is updated, the direct solution of the 1D model recalculated via the proposed method, and the error criterion — the sum of squared differences between the model's results and the measured profile — computed. The proposed approach demonstrates its effectiveness for real-time applications, especially in vibration analysis, where rapid and precise strain reconstruction is essential for monitoring structural integrity. Finally, the performance of the proposed approach is illustrated through a finite element simulation.

2. STRAIN TRANSFER SIMPLIFIED 1D MODEL

Several studies have been conducted to develop a simplified 1D model of strain transfer in fiber optic sensors, all leading to the same form of the governing equation: a second-order differential equation with Dirichlet boundary conditions, incorporating the strain-lag parameter [5]. This parameter characterizes the cable by considering factors such as the radius, Young's modulus, Poisson's ratio for each layer of the fiber optic sensor, and its installation conditions within the structure. The installation conditions are described through a coefficient known as the stiffness coefficient, which captures the bonding between the cable layers and between the cable and the host material. The 1D model describing the transfer from the strain profile $u(x)$ in the host material to the strain profile $y(x)$ in the fiber optic is given by:

$$y''(x) - \beta^2 y(x) = -\beta^2 u(x) \tag{1a}$$

$$y(x_0) = y_0 \, , \, y(x_N) = y_L \tag{1b}$$

where β is a positive number denoting the cable's strain-lag parameter, x is the spatial coordinate along the structure, y_0 and y_L are boundary conditions at the two ends of the structure corresponding to $x = x_0$

and $x = x_N$. The fiber optic produces measurements at some finite resolution, corresponding to equi-spaced points $x_0, x_1, x_2, \ldots, x_N$ (Fig.1).

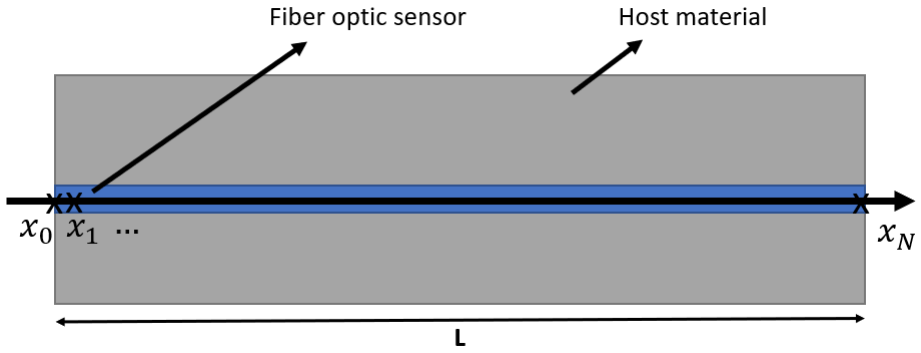

Figure 1: A representative structure equipped with a fiber optic sensor

3. AN EFFICIENT METHOD FOR SOLVING THE EQUATION OF THE STRAIN TRANSFER MODEL

The numerical solution of ordinary differential equations is usually based on ODE solvers, typically using Runge–Kutta methods, which integrate the equation from one end to the other, starting from the boundary conditions specified at a single end, known as Cauchy boundary conditions. Since the characteristic polynomial of the fiber optic 1D model (1) has two poles of opposite signs, namely $\pm\beta$, its solution in either of the two directions has a diverging tendency, causing numerical instability. Standard ODE solvers are unsuitable in this case, due to the numerical instability and the two-point boundary conditions specified in (1). The solution proposed in this section overcomes the two difficulties by decomposing the second order two-point boundary value problem into two first order Cauchy problems. This approach is an alternative to the Galerkin method [10], which transforms a differential equation to a discrete problem by applying linear constraints determined by finite sets of basis functions.

3.1. Decomposition into a system of two first-order equations

The decomposition of the second-order differential equation Eq.(1) into the sum of two first-order equations is based on its linear nature. Consider the two first-order equations

$$z_1'(x) = \beta z_1(x) - \frac{\beta}{2} u(x) \tag{2a}$$

$$z_2'(x) = -\beta z_2(x) + \frac{\beta}{2} u(x) \tag{2b}$$

$$z_1(x_N) = 0, \quad z_2(x_0) = 0 \tag{2c}$$

where $z_1(x)$ and $z_2(x)$ are two scalar variables. It is straightforward to check that, for any pair of solutions $z_1(x)$ and $z_2(x)$ satisfying respectively (2a) and (2b), the sum $y(x) = z_1(x) + z_2(x)$ satisfies the second order equation (1a). For the moment, the boundary conditions in (1b) are not yet taken into account.

Let us first consider the particular solution of (2b) specified by its boundary condition in (2c), namely $z_2(x_0) = 0$. It is given by

$$z_2(x) = \frac{\beta}{2} \int_{x_0}^{x} e^{-\beta(x-s)} u(s) ds, \text{ for } x \in [x_0, x_N]. \tag{3}$$

In this integral is the convolution between $e^{-\beta x}$ and $u(x)$. The fact that $\beta > 0$ ensures that the convolution is bounded for any bounded $u(x)$ (even for infinitely large $[x_0, x_N]$, i.e., when $x_N \to \infty$). More

importantly, when the integral is numerically computed, the decreasing exponential function $e^{-\beta x}$ when x increases avoids accumulation of numerical rounding errors.

For the other first order equation (2a), in order to obtain the same numerical stability, it is solved with the boundary condition $z_1(x_N) = 0$, also specified in (2c). As x_N is at the right side end of the interval $[x_0, x_N]$, equation (2a) is solved from right to left, yielding

$$z_1(x) = -\frac{\beta}{2} \int_{x_N}^{x} e^{\beta(x-s)} u(s) ds, \text{ for } x \in [x_0, x_N]. \tag{4}$$

This time the function $e^{\beta x}$ increases when x increases. In other words, $e^{\beta x}$ is decreasing when x decreases. For this reason the integration is computed backwards, from right to left over $[x_0, x_N]$, so that it is numerically stable, in a way similar to the previous case.

3.2. Adjusting the boundary conditions

Again due to the linearity of (1a), its boundary conditions specified in (1b) can be taken into account by adding more terms to $z_1(x) + z_2(x)$. Let

$$z_3(x) = e^{-\beta(x_N - x)} \tag{5a}$$

$$z_4(x) = e^{-\beta(x - x0)}. \tag{5b}$$

and again it is straightforward to check that

$$y(x) = z_1(x) + z_2(x) + c_1 z_3(x) + c_2 z_4(x) \tag{6}$$

satisfies (1a), with any scalar real coefficients c_1 and c_2.

The two coefficients c_1 and c_2 are chosen to satisfy the boundary conditions specified in (1b). It is achieved by solving for c_1 and c_2

$$\begin{cases} y_0 - z_1(x_0) = c_1 z_3(x_0) + c_2 z_4(x_0), \\ y_L - z_2(x_N) = c_1 z_3(x_N) + c_2 z_4(x_N). \end{cases} \tag{7}$$

3.3. Summary

Given the profile of $u(x)$ for $x \in [x_0, x_N]$, the value of β, and the boundary values y_0 and y_L, the efficient solution of the fiber optic 1D model (1) consists of the following steps

1. Compute $z_2(x)$ with (3) and $z_1(x)$ with (4).
2. Compute $z_3(x)$ and z_4 with (5).
3. Solve (7) for c_1 and c_2.
4. Compute $y(x)$ with (6), which is the solution of the fiber optic 1D model (1).

In practice, the profile of $u(x)$ is usually specified as a sequence $u(x_0), ..., u(x_N)$. Typically it is linearly interpolated to compute the integrals in (3) and (4).

4. RESOLUTION OF THE INVERSE PROBLEM

The previous section presented an efficient solution to compute $y(x)$ – the strain profile corresponding to a fiber optic sensor measurement – from $u(x)$, the strain profile in the host material. It is referred to as the direct problem. This section considers the inverse problem, consisting of computing $u(x)$ from $y(x)$.

In practice, a fiber optic sensor provides measurements corresponding to $y(x)$, which is the strain profile in the core of the fiber. However, the useful information is the strain profile in the host material, that is $u(x)$. It is thus important to solve the inverse problem.

By discretizing the interval $[x_0, x_N]$, the inverse problem consists in computing the sequence $u(x_0), ...,$ $u(x_N)$ from a measurement sequence $y(x_0), ..., y(x_N)$, given the value of β. Due to the large number of unknowns $u(x_0), ..., u(x_N)$, it is necessary to regularize the inverse problem. For numerical efficiency, let us decompose $u(x)$ as a linear combination of Gaussian functions. This approximation allows $u(x)$ to be represented as a weighted sum of Gaussian functions $(\phi_k)_{k=0,...,n}$, each centered at specific points b_k. $u(x)$ is expressed as:

$$u(x) = \sum_{k=0}^{n} a_k \phi_k(x), \text{ where } \phi_k = e^{-\left(\frac{x-b_k}{s}\right)^2} \tag{8}$$

b_k represents the centers and s controls the width of each Gaussian. A smaller s results in a more localized function, while a larger s spreads the function out. This approach effectively captures the strain's variation along the length while reducing the degrees of freedom by representing the strain profile with fewer parameters (using the coefficients $(a_k)_k$).

The solution to the inverse problem involves iteratively solving the direct problem while minimizing an error criterion. The objective is to adjust the parameters $(a_k)_k$ to minimize the following error function:

$$J(a) = \min_{a} \sum_{i}^{N} |y(x_i) - \hat{y}(x_i)|^2 \tag{9}$$

where $a = [a_1, a_2, \ldots, a_n]^T$ is the vector composed of the coefficients a_k's. $y(x_i)$ represents the measured strain at discrete points x_i, and $\hat{y}(x_i)$ is the strain profile computed using the profile of u (with the current values $(a_k)_k$ at each iteration, as defined in Eq.(8)) and the strain-lag parameter, via the proposed method for solving the direct problem. This minimization process identifies the optimal parameters $(a_k)_k$ that best match the measured data while benefiting from the stability and efficiency of the proposed method. To achieve this, the optimization is performed using a Newton-based trust-region method, which effectively balances convergence speed and robustness.

5. VALIDATION USING A FINITE ELEMENT SIMULATION

This section presents the results of a finite element simulation for a 4-point bending test on a concrete beam. The beam has dimensions of 2000 mm in length, 200 mm in width, and 200 mm in height, with material properties of Young's modulus = 37 GPa and Poisson's ratio = 0.2. To create a strain gradient, a defect is introduced at the center near the top, with dimensions as shown in Fig.2. The beam is subjected to a 10 kN force applied at the level of the steel supports at the top. The model is meshed using tetrahedral elements, each with an edge length of 10 mm. The strain profile along the green line, positioned 20 mm from the bottom and denoted as u, is extracted from the simulation, providing 200 data points along the 2000 mm length of the beam. This scenario is then analyzed as if a fiber optic sensor was integrated at this level. The proposed sensor is a robust, four-layered steel-reinforced cable with a diameter of 2 mm. The properties of the cable, chosen as detailed in Table 1, are used to compute the strain-lag parameter based on the formulation for four-layered systems, as described in [5], resulting in a value of $\beta = 8.5$ m^{-1}. The measured strain profile along this cable, denoted as y, can be obtained by solving the differential equation in Eq. (1) using the proposed method in Section 3, with the extracted profile u and a strain-lag value of $\beta = 8.5$ m^{-1}. Fig.3(a) shows the effect of the strain transfer occurring between the host material and the fiber optic sensor. To better reflect practical conditions, Gaussian measurement noise with a mean of 0 and a standard deviation of 4 is added to the calculated profile, y, resulting in a noise that does not exceed ± 14 μm/m.

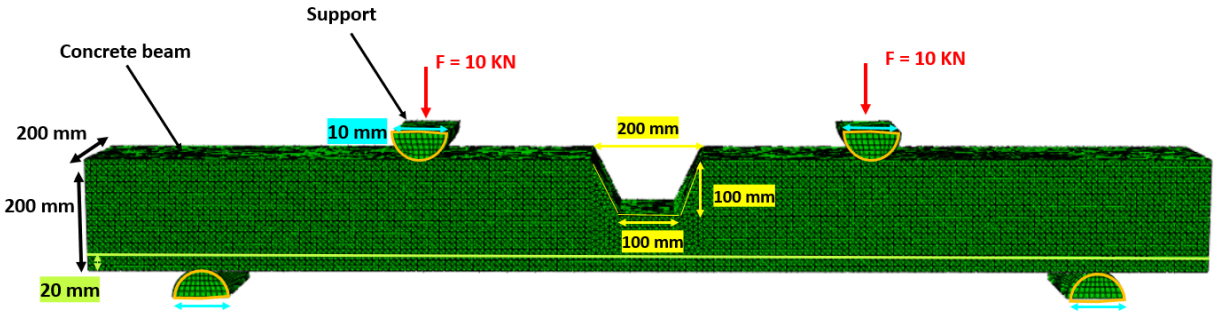

Figure 2: 4-Point bending test of a beam with a central defect

Table 1: Fiber optic sensor's geometric and mechanical properties

Layer	Radius [mm]	Young modulus [GPa]	Poisson's ratio	Stiffness coefficient [MPa/mm]
Optical fiber	0.06	70	0.3	10
Coating 1	0.12	1	0.4	10
Coating 2	0.77	200	0.3	10
Coating 3	1	4	0.4	10

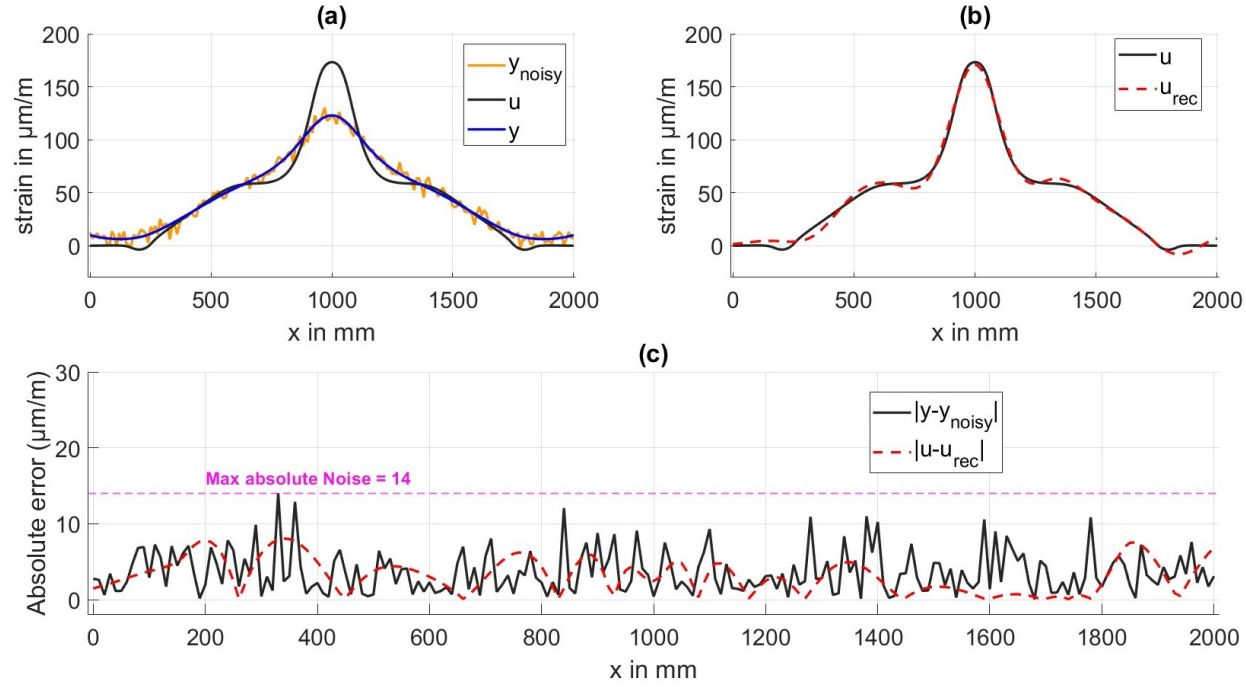

Figure 3: (a) Strain profiles in the host material, calculated strain in the optical fiber, and its noisy measurement. (b) Comparison between extracted and reconstructed strain profiles in the host material.(c) Comparison between absolute error and absolute noise.

The noisy strain profile, y_{noisy}, is used to solve the inverse problem and reconstruct the actual strain profile in the host material. To achieve this, the reconstructed profile, u_{rec}, is interpolated using a Gaussian basis function, as described in Eq. (8), with a limited number of Gaussians set to 15 and a standard deviation of $s = 350$. The coefficients $(a_k)_k$ are then estimated by minimizing the error criterion defined in Eq. (9), using the proposed method for solving the direct problem. Note that various choices for the number of Gaussians and the standard deviation could achieve an accurate reconstruction. However, selecting a

small number of Gaussians in this case was beneficial for reducing computational time while preserving accuracy.

To assess the effectiveness of the proposed method, the computed value u_{rec} is compared to u in Fig. 3(a), while the absolute error $|u - u_{\text{rec}}|$ is compared to the absolute noise in Fig. 3(b). The results show good agreement between the reconstructed and actual profiles in the host material, demonstrating the method's efficiency. Moreover, the absolute error remains within the same order of magnitude as the noise, implying high accuracy. Additionally, the computational time remains under 0.01s, indicating low time cost. This makes the approach particularly suitable for vibration analysis.

6. CONCLUSIONS

In conclusion, this paper presents an efficient and numerically stable method for solving the direct problem of the strain transfer model and the associated inverse problem. The proposed approach not only ensures high accuracy and computational efficiency. Fast computation is critical in vibration analysis because real-time monitoring often involves continuous data collection, where any delay in processing could lead to missed events and inaccurate results. By solving the inverse problem efficiently, the method significantly enhances real-time monitoring capabilities. It opens the door for using optical fiber sensors in vibration analysis, as their high spatial resolution and ability to monitor large areas can now be leveraged in real-time applications.

REFERENCES

[1] Peter Cawley. Structural health monitoring: Closing the gap between research and industrial deployment. *Structural Health Monitoring*, 17:1225–1244, 2018.

[2] Mudabbir Badar Bo Liu Benjamin T. Chorpening Michael P. Buric Paul R. Ohodnicki Ping Lu, Nageswara Lalam. Distributed optical fiber sensing: Review and perspective. *Appl. Phys. Rev*, 6: 41302, 2019.

[3] Ali Masoudi, Timothy Lee, Martynas Beresna, and Gilberto Brambilla. 10-cm spatial resolution distributed acoustic sensor based on an ultra low-loss enhanced backscattering fiber. *Opt. Continuum*, 1(9):2002–2010, Sep 2022.

[4] Farhad Ansari and Yuan Libo. Mechanics of bond and interface shear transfer in optical fiber sensors. *Journal of Engineering Mechanics*, 124:385–394, 1998.

[5] X. Chapeleau and A. Bassil. A general solution to determine strain profile in the core of distributed fiber optic sensors under any arbitrary strain fields. *Sensors*, 21, 2021.

[6] Feng Liu, Qianen Xu, and Yang Liu. Strain data correction of distributed optical fiber sensors using strain transfer model with variable shear lag parameters. *Automation in Construction*, 140:104311, 2022.

[7] Xing Zheng, Bin Shi, Cheng Cheng Zhang, Yijie Sun, Lei Zhang, and Heming Han. Strain transfer mechanism in surface-bonded distributed fiber-optic sensors subjected to linear strain gradients: Theoretical modeling and experimental validation. *Measurement*, 179:109510, 2021.

[8] Wenbo Du, Xing Zheng, Bin Shi, Mengya Sun, Hao Wu, Weida Ni, Zhenming Zheng, and Meifeng Niu. Strain transfer mechanism in surface-bonded distributed fiber optic sensors under different strain fields. *Sensors 2023, Vol. 23, Page 6863*, 23:6863, 2023.

[9] Mira Kabbara, Xavier Chapeleau, Qinghua Zhang, and Frédéric Bourquin. Numerical evaluation of strain transfer model for steel-reinforced optical fiber cable embedded in a cylindrical concrete beam with two void inclusions. *EPJ Web of Conferences*, 305:00021, 2024.

[10] Alfio Quarteroni, Riccardo Sacco, and Fausto Saleri. Numerical mathematics. 37, 2007.